Huiyang Fei

Amit Abraham

Mechanical and Aerospace Engineering,
School for Engineering of Matter,
Transport and Energy,
Fulton Schools of Engineering,
Arizona State University,
Tempe, AZ, 85287-8706

Nikhilesh Chawla

Mechanical and Aerospace Engineering,
Materials Science and Engineering,
School for Engineering of Matter,
Transport and Energy,
Fulton Schools of Engineering,
Arizona State University,
Tempe, AZ, 85287-8706

Hanqing Jiang[1]

Mechanical and Aerospace Engineering,
School for Engineering of Matter,
Transport and Energy,
Fulton Schools of Engineering,
Arizona State University,
Tempe, AZ, 85287-8706
e-mail: hanqing.jiang@asu.edu

Evaluation of Micro-Pillar Compression Tests for Accurate Determination of Elastic-Plastic Constitutive Relations

The micro-pillar compression test is emerging as a novel way to measure the mechanical properties of materials. In this paper, we systematically conducted finite element analysis to evaluate the capability of using a micro-compression test to probe the mechanical properties of both elastic and plastic materials. We found that this test can provide an alternative way to accurately and robustly measure strain, and to some extent, stress. Therefore, this test can be used to measure some strain related quantities, such as strain to failure, or the stress-strain relations for plastic materials. [DOI: 10.1115/1.4006767]

Keywords: micro-pillar compression, finite element analysis, elastic, plastic

1 Introduction

Understanding deformation behavior of materials requires knowledge of the local stress-strain behavior of individual microstructural phases and constituents. For example, the deformation behavior of dual phase steels is controlled by the martensite constituent and ferrite. In Sn-rich alloys used in electronic packaging, the mechanical properties of Cu_6Sn_5 intermetallic, Sn-Ag_3Sn eutectic, and pure Sn dendrites need to be measured. Such measurements cannot be made by making these materials in bulk form, because the microstructure, texture, and density of defects may change.

Quantifying the stress-strain behavior of small volumes is a challenge. Indentation techniques have been developed that enable the measurement of Young's modulus and hardness. Currently, the nanoindentation technique can achieve subnanometer displacement resolution and 1 nano-Newton force resolution, which makes the technique widely used to determine mechanical properties of small volumes [1]. Despite the popularity of the indentation test, it still has some intrinsic shortcomings. The main problem is that indentation involves a complex stress/strain field underneath the indenter depending on the specific tip geometry. Furthermore, extraction of uniaxial stress-strain constitutive relations, while possible, require complex iterative methods [1].

Recently, a variant on nanoindentation, called micropillar compression, has been developed. The technique uses a nanoindenter with a flat punch to compress a small cylindrical volume (1 μm diameter by 2 μm length cylinders) to obtain a uniaxial stress-strain behavior (Fig. 1(*a*)). Micropillars are machined by milling materials of interest using focused ion beam (FIB) (Fig. 1(*b*)) with diameters ranging from 200 nm to a few μm [2] within a single phase of the constituent. Figure 1(*c*) shows a pillar of Cu_6Sn_5 intermetallic milled by FIB [3]. Various materials have been tested by this technique, including Mg, Ta, and Cu_6Sn_5 [3–6]; other studies have focused on simulations based on crystal plasticity [7] and dislocation dynamics [8].

Compared with the micro-indentation test, micro-compression has the obvious advantage of a relatively uniform stress/strain field. However, since micro-compression test is a new technology to measure the strain-strain relation, there is no standard yet. Moreover, there are several experimental variables, however, that may affect accurate measurements of strain and stress. These variables include the aspect ratio α (the ratio of height h and diameter d of the pillar), size of substrate below the pillar, taper angle θ (>0) (the angle between the tangent of wall and axis of the pillar), fillet angle, misalignment between the pillar axis and the compression direction, and stiffness of the substrate. It also must be realized that the presence of the substrate leads this problem to become complicated and many straightforward analytical analyses cannot be simply applied.

The effect of some of these variables can be intuitively understood. For example, for a compliant substrate, the pillar will sink upon compression and the majority of the deformation will be carried by the substrate instead of the pillar, which will lead to inaccurate measurement of the pillar deformation. This sink-in effect may be magnified for pillars with a large aspect ratio and suppressed for pillars with a large taper angle. A larger aspect ratio may also lead to premature buckling of the pillars upon compression. This intuitive argument indicates that these factors may be coupled together to influence the accuracy of the experimental measurement. Zhang et al. [4] used the finite element method to study some of these effects, including aspect ratio, fillet angle, taper angle and misalignment for a pillar on a very thin substrate sitting on a rigid base.

In this paper, we have conducted systematic and parametric finite element analysis to evaluate the micro-compression test from several aspects, and propose methods to accurately calculate stress and strain with good correlation with experimentally measureable

[1]Corresponding author.

Manuscript received July 31, 2011; final manuscript received February 16, 2012; accepted manuscript posted May 3, 2012; published online September 17, 2012. Assoc. Editor: Daining Fang.

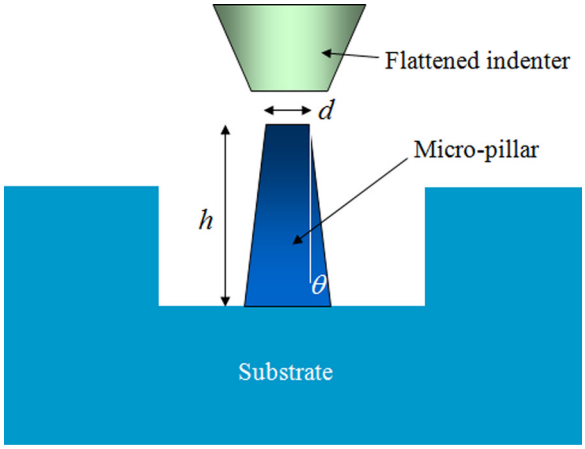

(a)

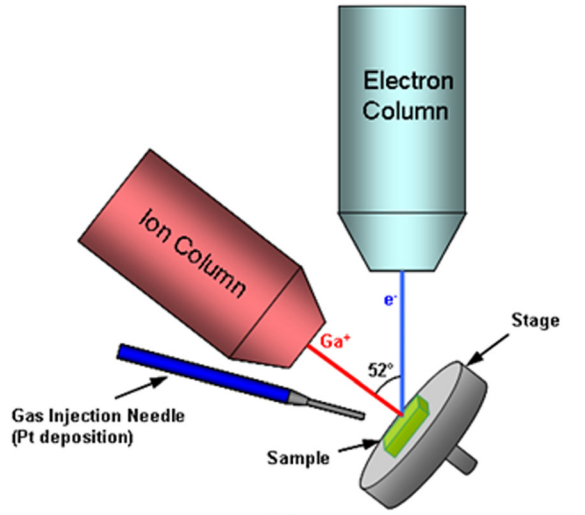

(b)

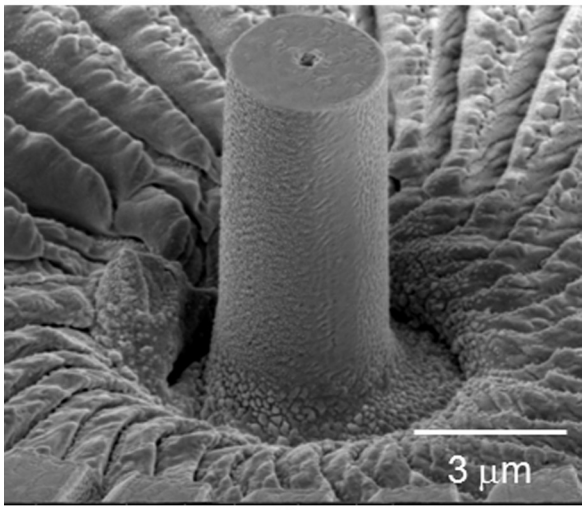

(c)

Fig. 1 (*a*) Schematic of the micro-pillar compression test, (*b*) schematic of focused ion beam (FIB), and (*c*) scanning electron microscopy (SEM) image of a micro-pillar on a single grain of Sn-Ag-Cu (SAC) alloy, with a taper angle of ~4 deg

quantities. The structure of the paper is as follows. We present our finite element model in Sec. 2 followed by a methodology on how the strain was measured in the micropillar. The deformations of the indenter, micro-pillar, and substrate are coupled together, so the purpose of the work presented in Sec. 3 is on a methodology on how to eliminate the influences of deformation of the substrate and indenter in the strain measurement. In Sec. 4, we considered factors that affect the micro-pillar stress measurement. The shape of the micro-pillar will cause a nonuniform stress field, which will make the stress calculation more difficult. The taper angle and aspect ratio effects are specifically evaluated in Sec. 4.

2 Finite Element Model

We have used an axisymmetric geometry to model the micro-compression test, as shown in Fig. 2(*a*). An indenter with radius, r_{indenter}, is included, although its deformation maybe very small, and modeled as an elastic material. r_{top} is the top radius of the pillar, θ is the taper angle, and h is the height of the pillar. The dimension of the substrate is $L \times L$. Figure 2(*a*) is not drawn to scale since the size of the substrate is about two orders of magnitude greater than that of the pillar. The pillar and substrate are the same material and can be elastic or plastic. The interface between the pillar and substrate is realized by sharing nodes. The prescribed displacement boundary condition $v = 0$ is applied at the bottom of the substrate to model the rigid base underneath the substrate. The axisymmetric boundary condition $u = 0$ is applied along the symmetric axis. Here u and v represent the displacements along the x and y directions, respectively. The surface-to-surface contact is assigned between the indenter and the top of the pillar and a prescribed pressure load p is applied on top of the indenter, so the axial compressive force is $f = \pi r_{\text{indenter}}^2 p$. The finite element analysis is conducted via the commercial finite element package ABAQUS/Standard (version 6.9). Axisymmetric 4-node continuum elements (CAX4) and 3-node elements (CAX3) are chosen for discretization. Mesh sensitivity is studied by reaching a convergent load/displacement curve extracted from the pillar region. A typical convergent mesh with about 200,000 elements is shown in Fig. 2(*b*), with the inset of the pillar region.

The range of geometric parameters used in the analyses are as follows: $r_{\text{indenter}} = 1\ \mu\text{m}$, $r_{\text{top}} = 0.5\ \mu\text{m}$, $\theta = 0 \sim 5$ deg, $\alpha = h/2r_{\text{top}} = 2 \sim 4$, $L = 10 \sim 70\ \mu\text{m}$. The elastic materials used for the pillars have Poisson's ratio 0.3 and Young's modulus ranging from 50 GPa to 400 GPa. The plastic material used here is that of a Sn-rich alloy with 3.5 wt.% Ag with Young's modulus 45.6 GPa, Poisson's ratio 0.3, and the experimentally determined stress-strain curve via tensile test for the plastic zone shown in Fig. 2(*c*).

3 Measurement of Pillar Strain

3.1 Indentation Depth and Sneddon's Correction. In this section, we discuss the measurement of pillar strain in the micro-compression test. It should be noted that the pillar strain cannot be directly measured in the micro-compression experiment. Instead, the measurable variable is the indentation depth, i.e., the displacement of the top surface of the indenter with respect to the rigid base underneath the substrate. In other words, the total displacement of the system, including indenter, pillar and substrate, is the directly measurable quantity, which is given by

$$\Delta x_{\text{total}} = \Delta x_{\text{ind}} + \Delta x_{\text{pillar}} + \Delta x_{\text{sub}} \tag{1}$$

where Δx_{total} is the indentation depth, Δx is the deformation of each part in the micro-compression test with subscripts "ind," "pillar," and "sub" denoting indenter, pillar, and substrate, respectively. The pillar deformation Δx_{pillar} is the quantity of interest, which needs to be accurately quantified by eliminating the deformations of indenter and substrate from the total displacement.

The deformation of the pillar into the substrate can be described by the work of Sneddon [9]. Sneddon [5] considered the sinking effect of a cylindrical punch indenting into an elastic half space,

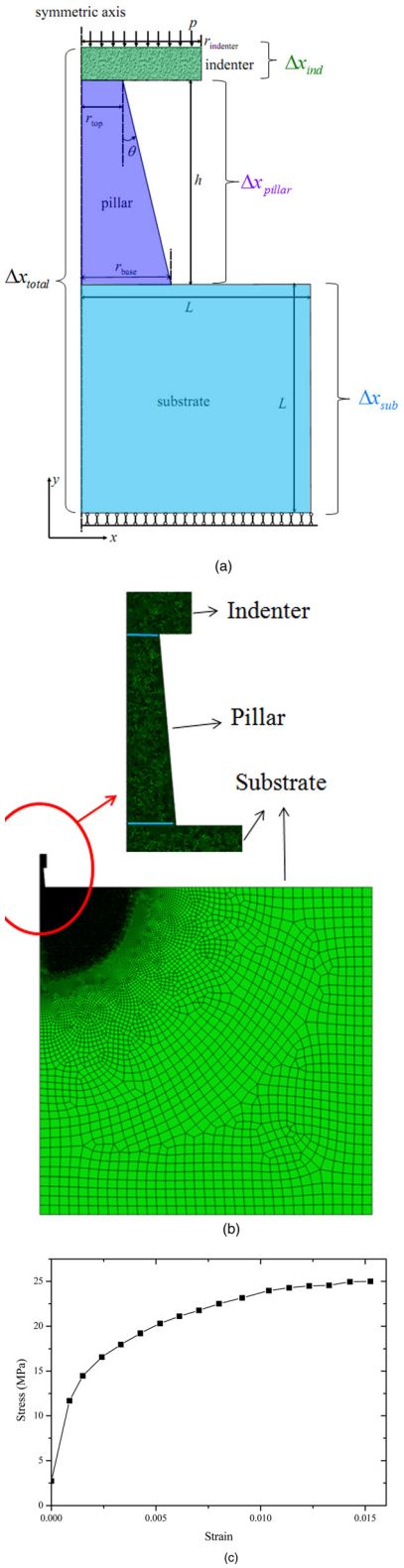

Fig. 2 (*a*) Schematic of axisymmetric model of the micro-pillar, (*b*) geometry and mesh of the finite element model, and (*c*) the stress-strain curve for the plastic material used in this study

and developed an analytical formula to calculate the compliance associated with the deformation of the half space material, which is given by

$$C_{\text{Sneddon}} = \frac{(1-\nu^2)\sqrt{\pi}}{2E\sqrt{A_p}} \tag{2}$$

where C_{Sneddon} is the compliance of the half-space material, E is the Young's modulus, ν is the Poisson's ratio, and A_p is the contact area between the punch and the half-space material. Equation (2) can be applied to the micro-compression test by assuming the punch to be the pillar and the half-space material to be either the indenter and/or substrate. Thus, the deformations of indenter and substrate are given in terms of their compliance by considering the system as series springs consisting of the indenter, pillar, and substrate,

$$\Delta x_{\text{ind}} = C_{\text{ind}} f, \quad \Delta x_{\text{sub}} = C_{\text{sub}} f \tag{3}$$

where $f = \pi r_{\text{indenter}}^2 p$ is the applied force on top of indenter and p is the pressure. The pillar deformation then can be given by [3,6,10]

$$\Delta x_{\text{pillar}} = \Delta x_{\text{total}} - \frac{(1-\nu_{\text{sub}}^2)\cdot f}{2E_{\text{sub}}\cdot r_{\text{base}}} - \frac{(1-\nu_{\text{ind}}^2)\cdot f}{2E_{\text{ind}}\cdot r_{\text{top}}} \tag{4}$$

where, r_{top} and r_{base} are the radius of the top and base surface of the pillar, respectively (Fig. 2(*a*)). A typical indenter used in the micro-compression test is made of diamond with Young's modulus of 1141 GPa and Poisson's ratio of 0.07 [9]. The substrate is normally the same material as the pillar. Although Sneddon's correction has been applied to the micro-compression tests (See, for example, Ref. [3]), its accuracy has not yet been evaluated since the assumptions in Sneddon's correction, e.g., half-space elastic material as the substrate, may not hold in micro-compression tests. The finite element analysis was conducted to evaluate the accuracy of Sneddon's correction in micro-compression tests.

In finite element analysis, the total displacement Δx_{total} is the displacement in the y-direction measured from to the top of the indenter to the bottom of the substrate (i.e., rigid-body support); Δx_{ind} is the difference in the y-direction displacement from the top to the bottom surfaces of the indenter; Δx_{pillar} is the displacement of the top surface of the pillar with respect to the bottom surface of the pillar, and Δx_{sub} is the deformation of the substrate. To differentiate from the Sneddon's correction, Δx_{pillar} in Eq. (4) is denoted as $\Delta x_{\text{pillar}}^{\text{Sneddon}}$ in the following. The contribution of each component to the total displacement is expressed by the deformation ratio given by

$$\begin{aligned} \text{pillar}\% &= \frac{\Delta x_{\text{pillar}}}{\Delta x_{\text{total}}} \\ \text{substrate}\% &= \frac{\Delta x_{\text{sub}}}{\Delta x_{\text{total}}} \\ \text{indenter}\% &= \frac{\Delta x_{\text{ind}}}{\Delta x_{\text{total}}} \end{aligned} \tag{5}$$

and

$$\text{Sneddon}\% = \frac{\Delta x_{\text{pillar}}^{\text{Sneddon}}}{\Delta x_{\text{total}}} \tag{6}$$

It should be noted that, here, we do not intend to compare with experiments but to evaluate the accuracy of the Sneddon's correction; therefore, all displacement components (i.e., Δx_{ind}, Δx_{sub}, Δx_{pillar}, and Δx_{total}) are calculated from the finite element analysis and $\Delta x_{\text{pillar}}^{\text{Sneddon}}$ is then computed based on Eq. (4).

The finite element model has a pillar with 3 μm in height and 0.5 μm in top radius as well as a large substrate with size of 50 μm × 50 μm. Figure 3(*a*) shows the deformation ratios for an elastic material with Young's modulus $E = 50$ GPa and Poisson's ratio $\nu = 0.3$. It is found that the pillar deformation contributes around 80% to the total displacement (i.e., indentation depth) and the substrate deformation is close to 20% of the total displacement. The substrate deformation, which is also referred to as pillar "sink-in," causes the error in deformation measurement. With the increase of the pressure applied on the indenter, these deformation

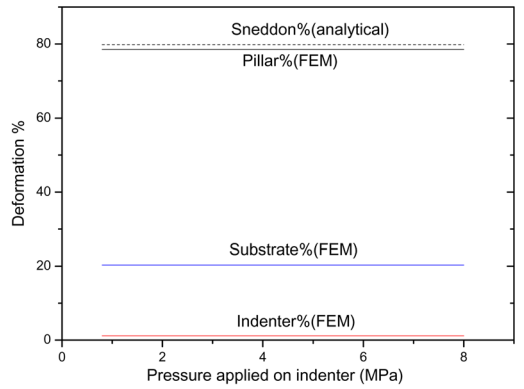

(a)

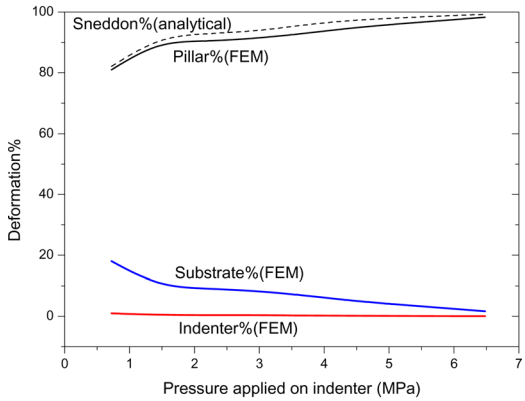

(b)

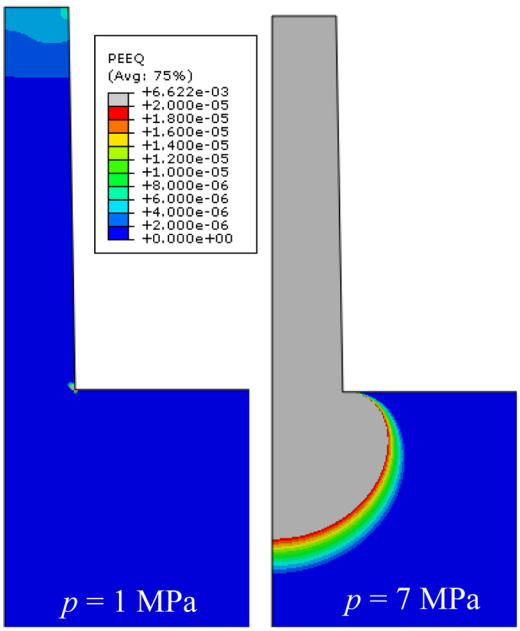

(c)

Fig. 3 The deformation percentage of pillar, substrate, and indenter for (*a*) elastic and (*b*) plastic materials. For elastic material, Young's modulus $E = 50$ GPa and Poisson's ratio $\nu = 0.3$. For plastic material, the stress-strain curve is given by Fig. 2(*c*). (*c*) Contours of equivalent plastic strain for a pillar subject to different pressure on top of the indenter (not shown here). The pressures are 1 MPa and 7 MPa for the left and right panels, respectively. The geometry of the micro-pillar compression in this figure is that the pillar is 3 μm in height and 0.5 μm in radius on a 50 μm × 50 μm substrate.

ratios for elastic materials remain constant as the system is linear and the deformations of all components increase proportionally with their relative ratios unchanged. It is also observed that the Sneddon's correction agrees fairly well with the finite element analysis, which suggests that Sneddon's correction can significantly reduce the error caused by pillar "sink-in".

Figure 3(*b*) shows a similar trend for the plastic material with constitutive model given by Fig. 2(*c*). The contribution from the indenter is negligible and the Sneddon's correction captures the trend of pillar deformation. Compared with the results for the elastic material, the deformation ratios for the plastic material are not constant. Specifically, with the increase of the applied pressure, the pillar displacement contribution increases while that for the substrate decreases. This can be explained by the total deformation being controlled by the equivalent plastic strain (PEEQ) in the pillar, as shown in Fig. 3(*c*). As the applied pressure increases from 1 MPa (left panel) to 7 MPa (right panel), the plastic zone in the pillar is enlarged significantly compared with that of the substrate. Therefore, the substrate carries less deformation as the pressure increases, which explains the decreasing trend of the substrate contribution as the pressure increases shown in Fig. 3(*b*).

The studies in this subsection show that Sneddon's correction is able to capture the pillar deformation for both elastic and plastic materials, though its accuracy is quantified further in the next subsections.

3.2 Accuracy of Sneddon's Correction. The accuracy of Sneddon's correction can be more precisely evaluated by the measurement of strain. The strain in the pillar, based on Sneddon's correction, is given by

$$\varepsilon_{\text{pillar}}^{\text{Sneddon}} = \frac{\Delta x_{\text{pillar}}^{\text{Sneddon}}}{h} \tag{7}$$

In the finite element analysis, we can measure the actual displacement of the pillar, so the strain is just given by

$$\varepsilon_{\text{pillar}} = \frac{\Delta x_{\text{pillar}}}{h} \tag{8}$$

We can then define the error in strain e as

$$e = \left| \varepsilon_{\text{pillar}}^{\text{Sneddon}} - \varepsilon_{\text{pillar}} \right| \tag{9}$$

In other words, $\varepsilon_{\text{pillar}}$ based on the finite element analysis can be considered the "reference strain" so the error in strain is simply the deviation of the Sneddon's correction from the reference strain.

Figure 4(*a*) shows the deviation in strain, e, as a function of applied pressure on the diamond indenter for elastic pillars (and substrates). In these studies, the height of the pillar is 3 μm, and the radius is 0.5 μm with taper angle of 0 deg. The size of the substrate is 50 μm by 50 μm and the diamond indenter is 1.0 μm in both radius and height. Four elastic materials are studied, with Young's modulus ranging from 50 GPa to 400 GPa and Poisson's ratio 0.3. Figure 4(*a*) shows that the strain error e increases linearly with the applied pressure. Materials with higher Young's modulus have relatively smaller strain error. All strain errors are on the order of 10^{-5}, i.e., the strain error is very small. This result clearly shows that Sneddon's correction provides a very accurate estimation of the pillar strain for elastic materials.

One should note that although the strain errors are negligible (on the order of 10^{-5}), the relative strain error may not be that small since the strain for the elastic materials are usually very small (on the order of 10^{-4} to 10^{-3}). The relative strain error is defined as

$$\eta = \left| \frac{\varepsilon_{\text{pillar}}^{\text{Sneddon}} - \varepsilon_{\text{pillar}}}{\varepsilon_{\text{pillar}}} \right| \tag{10}$$

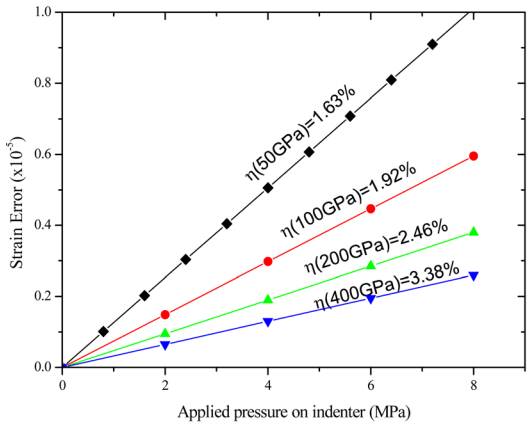

(a)

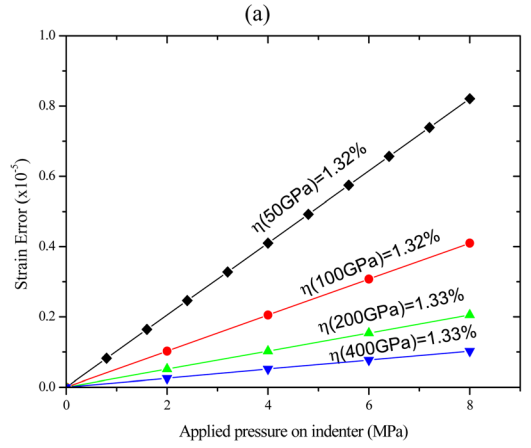

(b)

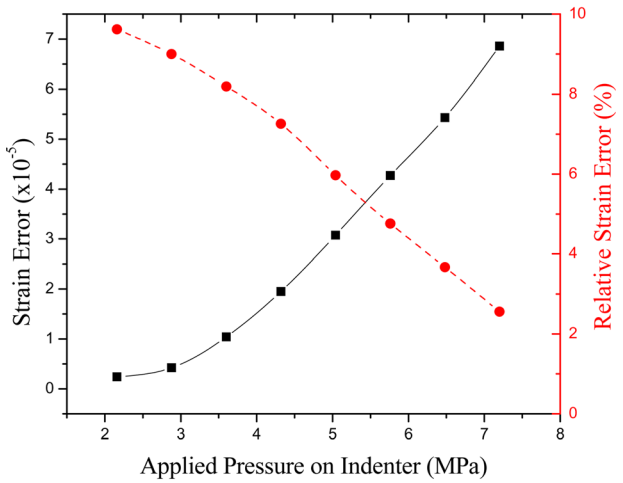

(c)

Fig. 4 Indenter effect on the strain measurement. Strain error and relative strain errors of elastic pillars when the pressure is applied on (*a*) a diamond intender, and (*b*) a rigid indenter. (*c*) Strain errors and relative strain errors for a plastic material with stress-strain curve given by Fig. 2(*c*) as input.

and also shown in Fig. 4(*a*). As one can expect, the relative strain error is on the order of 1%, which is three orders of magnitude larger than the strain error. Moreover, the relative strain error for materials with higher Young's modulus is surprisingly larger than that for materials with lower Young's modulus, which is opposite to the trend of strain errors. The explanation is related to one of the assumptions in Sneddon's correction, namely, the half-space substrate. The half-space substrate is always valid for the current pillar/substrate structure since the size of substrate is one order of magnitude larger than that of the pillar, but may not be applied to pillar/indenter. For pillars with relatively low modulus (e.g., 50 GPa) compared with the diamond indenter with modulus 1141 GPa, the half-space assumption is valid. However, 1 μm-high diamond indenter cannot be considered as a half-space substrate for pillars with higher modulus, such as 400 GPa. To verify the above explanation, we also show the strain errors and relative strain errors when the pressure is directly applied on the pillars, e.g., removing the effect the indenter, in Fig. 4(*b*). Clearly, the strain errors are about the same as that in Fig. 4(*a*), but the relative strain errors do not show significant difference for pillars with different modulus.

Figure 4(*c*) shows the strain errors and relative strain errors for a plastic material with the stress-strain curve given in Fig. 2(*c*). The strain errors are also very small, on the order of 10^{-5}. A different trend on relative strain error is observed, which varies from 2% to 10% for plastic materials, while for elastic materials it is a constant (Fig. 4(*a*)). The explanation is that the contribution of the deformation of the substrate deformation to the total deformation decreases with an increase in pressure due to large amount of plastic deformation in the pillar, as discussed in Fig. 3(*b*).

The above study leads us to conclude that the Sneddon's correction can provide a very accurate measurement on the pillar strain, particularly when the pillar materials are much softer than the indenter or the pillar is much smaller in volume relative to the indenter.

3.3 Substrate Effect. The previous results, specifically Figs. 3(*a*), 3(*b*), and 4, show that the deformation of the indenter is negligible and has very small effects on the accuracy of the measurement of strain in the pillar. We can hypothesize, then, that the deformation of the substrate can introduce significant errors in strain measurement. In this section, we evaluate the effect of the substrate on deformation behavior of the pillar. In the ideal scenario, i.e., where pillar rests on top of a rigid base, there is no "sink-in effect."

To quantify how the substrate size affects the strain measurement, substrates with various sizes, ranging from 10 μm × 10 μm to 70 μm × 70 μm, are considered. A pillar with 3 μm in height, 0.5 μm in radius and 0 deg in taper angle is used. Figure 5(*a*) shows the results for an elastic material with Young's modulus 50 GPa and Poisson's ratio 0.3. For a substrate with smaller size; for example, 10 μm × 10 μm (i.e., the leftmost point in Fig. 5(*a*)), the strain error is smaller compared with that for substrates with larger size. As the size of the substrate increases, the strain error reaches a plateau, which also is reasonably small (on the order of 10^{-4}). One of the assumptions in the Sneddon's correction, namely half-space substrate, is responsible for the convergence of the strain error as the size of the substrate increases. This study indicates that for elastic materials, the substrate effect is negligible. It is not necessary to devote efforts to eliminate the substrate in order to get better strain measurement. Even if the substrate is large, the error from the Sneddon's correction converges to a reasonably small level (on the order of 10^{-4}). Figure 5(*b*) shows the substrate effect for plastic materials. The material model is given by Fig. 2(*c*) and the same geometry in Fig. 5(*a*) is used. A similar trend is observed, i.e., the strain errors converge to a very small value.

The studies in this subsection conclude that the Sneddon's correction can provide very accurate strain measurement no matter the size of the substrate and the material type.

3.4 Aspect Ratio and Taper Angle Effect. In this section, the influence of a pillar shape, namely, aspect ratio and taper angle, on the strain measurement is described.

The aspect ratio is defined as

$$\alpha = \frac{h}{2r_{\text{top}}} \tag{11}$$

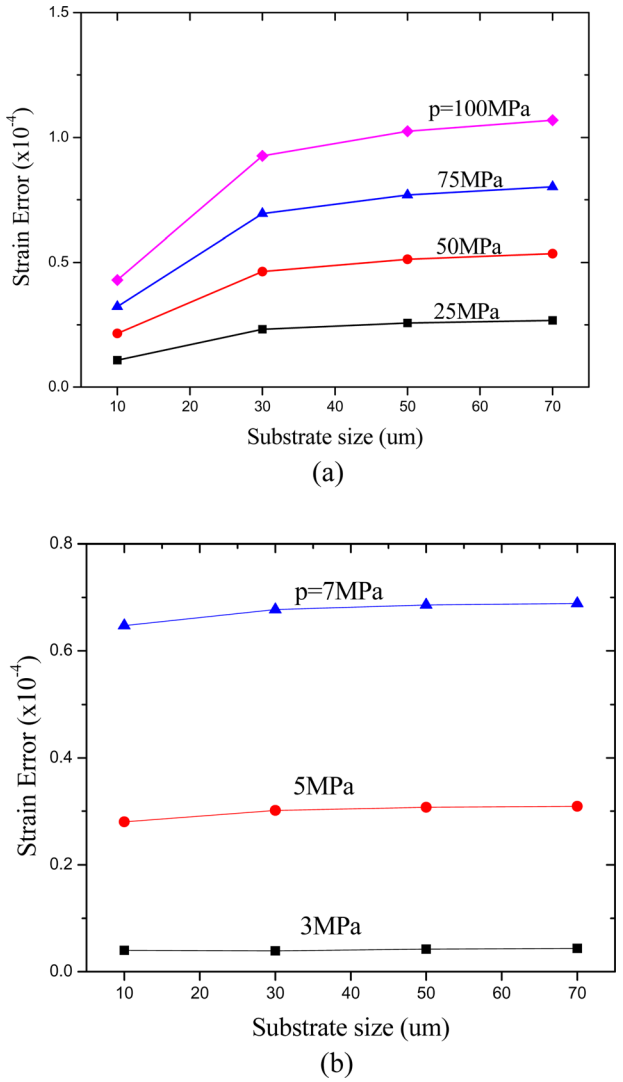

Fig. 5 Substrate size effect on the strain measurement, for (*a*) an elastic material with Young's modulus 50 GPa and Poisson's ratio 0.3, and (*b*) a plastic material with stress-strain curve given by Fig. 2(*c*)

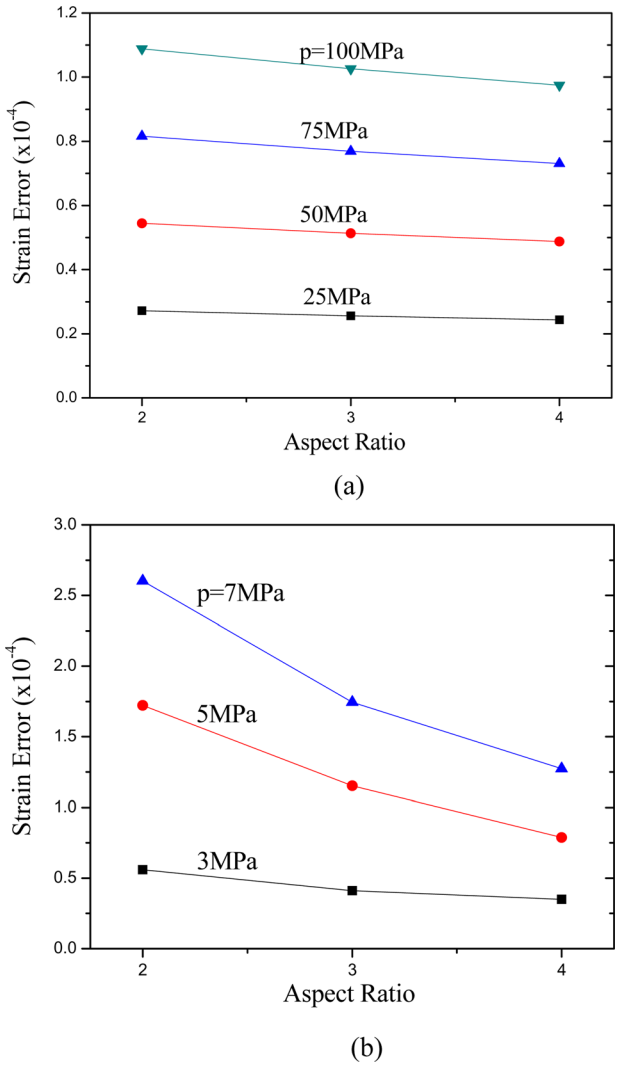

Fig. 6 Aspect ratio effect on the strain measurement, for (*a*) an elastic material with Young's modulus 50 GPa and Poisson's ratio 0.3, and (*b*) a plastic material with stress-strain curve given by Fig. 2(*c*)

Oftentimes, the pillar radius is fixed due to the resolution of micro-machining, such that the aspect ratio can be controlled by changing the pillar height. In the following finite element analysis, a pillar with $r_{top} = 0.5$ μm and 0 deg taper angle and a 50 μm $\times$ 50 μm substrate (a larger enough substrate having convergent results from Fig. 5) is used. The aspect ratio is varied from 2 to 4, which corresponds to a pillar with height from 2 to 4 μm. These parameters agree well with the present experiments. Figure 6(*a*) shows the results for an elastic material with $E = 50$ GPa, $\nu = 0.3$, and Fig. 6(*b*) gives the results for a plastic material with constitutive relation shown in Fig. 2(*c*). These results illustrate that the aspect ratio does not play an important role on the accuracy of the strain measurement using the Sneddon's correction, since the strain errors are insignificant. This trend can be explained in the following. When the pillar radius is fixed, there are only two length-dimension parameters, pillar height h and substrate dimension L, the ratio of which is a nondimensional parameter, h/L. This parameter is similar to the signal-to-noise ratio since the pillar is of our interest and the effect of substrate should be eliminated. High aspect ratio, or taller pillar, will provide "stronger signal" and just leads to smaller strain errors.

In addition to the aspect ratio, another parameter used to describe a pillar is its taper angle θ (Fig. 2(*a*)). An ideal micro-pillar is perfectly straight, although a slight taper angle exists for most micro-pillars due to the nature of micro-machining with the focused ion beam. The taper angle leads to a question mark on the strain measurement since the Sneddon's correction is based on a straight cylindrical punch and not a tapered pillar. Finite element analysis was conducted to evaluate the effect of the taper angle. The taper angles ranged from 0 deg to 5 deg to match with that of typical experiments. The pillar geometry is that 3 μm in height and 0.5 μm in top radius. The size of the substrate is 50 μm $\times$ 50 μm.

Figure 7(*a*) represents the results for an elastic material with $E = 50$ GPa and $\nu = 0.3$. Despite the fact that the Sneddon's correction is only valid for straight pillars (i.e., 0 deg taper angle), the effect of taper angle is not significant. As the taper angle is limited to 5 deg from the practical point of view, the strain error is within 10^{-4}. The results for a plastic material (given by Fig. 2(*c*)) are shown in Fig. 7(*b*), which is opposite to that of the elastic material. Smaller strain errors for tapered plastic pillar can be qualitatively understood this way. The Sneddon's correction was originally derived to eliminate the sink-in effect for an elastic material punching another elastic material. A relatively larger strain error for plastic materials, even for smaller pressure and 0 deg taper angle, indicates that the sink-in effect for plastic materials are not eliminated as much as that for elastic materials. As the

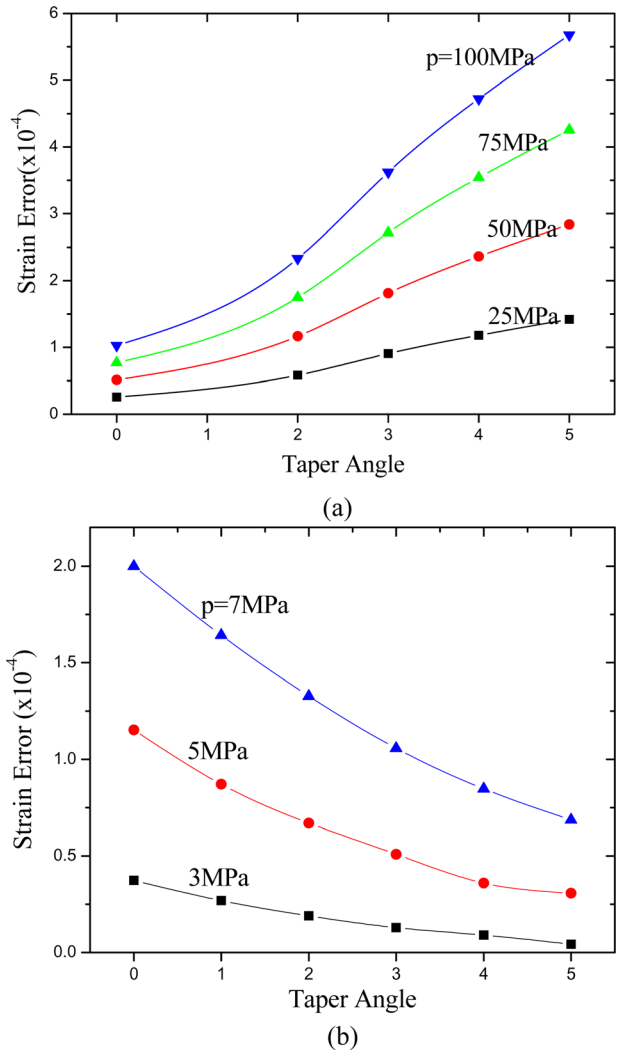

Fig. 7 Taper angle on the strain measurement, for (*a*) an elastic material with Young's modulus 50 GPa and Poisson's ratio 0.3, and (*b*) a plastic material with stress-strain curve given by Fig. 2(*c*)

taper angle increases, the base radius of the pillar r_{base} increases, which inhibits the sink-in effect and explains the decreasing trend of the strain errors shown in Fig. 7(*b*).

The studies in this section conclude that the Sneddon's correction works well for pillars with low or high aspect ratios and with or without taper angels, no matter whether the materials are elastic or plastic.

4 Measurement of Pillar Stress

The stress calculation in the micro-compression test is based on the assumption of uniform stress state in the pillar, which is also one of the advantages of micro-compression test compared with micro-indentation where a complex stress state is involved. The test is load-controlled, i.e., the pressure applied on top of the indenter p is prescribed. Then the stress can be calculated as

$$\sigma = \frac{r^2_{\text{indenter}}}{r^2_{\text{top}}} p \tag{12}$$

This section will evaluate the accuracy of this stress calculation.

4.1 Taper Angle Effect. As mentioned above, a taper angle exists for most micro-pillars, which causes the constitutive relation inaccurate and deviating from the real one. Figure 8(*a*) compares the stress field of two pillars, a straight one ($\theta = 0$ deg) and a tapered one ($\theta = 5$ deg). The material is elastic with $E = 50$ GPa and $\nu = 0.3$; the pillar geometry is 3 μm in height and 0.5 μm in top radius; the substrate size is 50 μm $\times$ 50 μm. A 30 MPa pressure is applied on top of the indenter, and the contour shows typical stress fields for a perfectly straight pillar and a tapered pillar. The stress state in the straight pillar (left panel) is fairly uniform so that Eq. (12) can be applied. However, for the tapered pillar (right panel), the stress is very nonuniform. Thus, we need to develop a means to calculate the pillar stress for tapered pillars to reflect the nonuniformity of the pillar stress.

Among many different ways to definite the average stress, the followings ones are very straightforward. The first one is to use the average cross sectional area of the pillar, given by

$$\sigma^{(1)} = \frac{r^2_{\text{indenter}}}{\frac{1}{2}\left(r^2_{\text{top}} + r^2_{\text{base}}\right)} p \tag{13}$$

the second one is to use the average pillar radius, given by

$$\sigma^{(2)} = \frac{r^2_{\text{indenter}}}{\left(\frac{r_{\text{top}} + r_{\text{base}}}{2}\right)^2} p \tag{14}$$

and the third one is to use the average stress at the top and bottom surface, given by

$$\sigma^{(3)} = \frac{1}{2}\left(\frac{r^2_{\text{indenter}}}{r^2_{\text{top}}} + \frac{r^2_{\text{indenter}}}{r^2_{\text{base}}}\right) p \tag{15}$$

These three means of calculating pillar stress all degenerate to Eq. (12) when the pillar is straight. We must admit that all these definitions are just geometric rather than physical since we try to find an empirical means to average out nonuniformly distributed stress field (as shown in Fig. 8(*a*)). Finite element analyses are conducted to evaluate these different stress measurements. The pillar geometry is 3 μm in height and 0.5 μm in top radius; the substrate size is 50 μm $\times$ 50 μm. A 600 MPa pressure is applied on top of the indenter. Two extreme cases, pillars with 0 deg to 5 deg taper angles are studied.

Firstly, an elastic pillar is studied. The input material parameters are $E = 50$ GPa and $\nu = 0.3$. The material property of interest is the Young's modulus that can be extracted from the finite element analysis via

$$E_{FEM} = \frac{\sigma^{(i)}}{\varepsilon^{\text{Sneddon}}_{\text{pillar}}}, \quad i = 1, 2, 3 \tag{16}$$

Here the pillar strain based on Sneddon's correction (Eq. (7)) is used as this strain is the one that can be obtained from the experiment. In other words, Eq. (16) expressed a measurable Young's modulus from experiments. Figure 8(*b*) shows that the measureable Young's moduli are higher than the input modulus (50 GPa) when the taper angle is present. Even for a straight pillar (0 deg taper angle), the slight nonuniformity of the pillar stress (left panel of Fig. 8(*a*)) makes the measureable Young's modulus a bit off from the input. Here we must point out that since the stress state is nonuniform so that the measured stress-strain curve is not the direct constitutive relation and thus its slope has to be carefully evaluated in order to obtain the Young's modulus. Therefore, the micro-compression test cannot be accurately applied to measure the Young's modulus.

We also studied a plastic pillar. The input stress-strain curve is given by Fig. 2(*c*) and is represented as black squares in Fig. 8(*c*). When taper angle is 0 deg, finite element analysis can reproduce the input stress-strain curve. When the taper angle is 5 deg, the

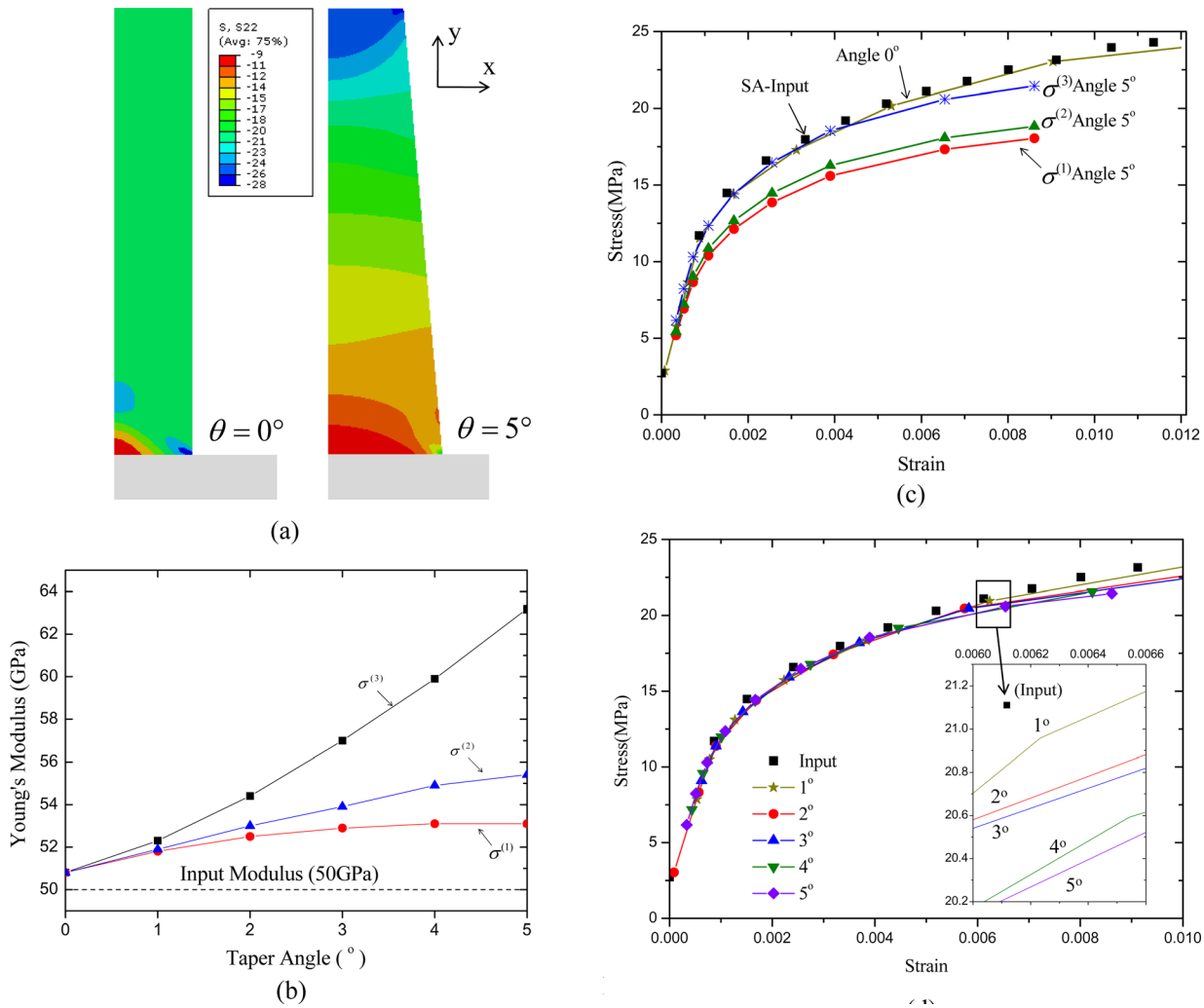

Fig. 8 (*a*) Contours of pillar stress for a straight pillar ($\theta = 0$ deg) and a tapered one ($\theta = 5$ deg). The material is elastic, $E = 50$ GPa and $\nu = 0.3$; the pillar geometry is 3 μm in height and 0.5 μm in top radius. The substrate size is 50 μm × 50 μm (not completely shown). (*b*) Taper angle effect of an elastic pillar on measuring the Young's modulus. (*c*) Evaluation of different stress measurement for plastic pillars with different taper angles. (*d*) Taper angle effect of stress measurement on plastic pillars using Eq. (15). Black square points are stress-strain input from Fig. 2(*c*).

stress defined by Eq. (15), i.e., averaging stresses at the top and bottom surface of the pillar, gives the most accurate result when the strain is less than 0.4% for the Sn-Ag modeled. As the strain increases, the stress given by Eq. (15) also starts to deviate from the input stress-strain curve. This study shows that the stress defined by Eq. (15), to some extent, has a certain level of accuracy. Figure 8(*d*) gives the measured stresses using the averaging based on Eq. (15), for pillars with taper angles from 1 deg to 5 deg. It clearly shows that the taper angles make the stress measurement less accurate.

4.2 Aspect Ratio Effect. Another concern is about how the aspect ratio of the pillar affects the accuracy of stress measurement. In the following finite element analysis, the pillars with aspect ratios of 2, 3, and 4, and top radius of 0.5 μm on a 50 μm × 50 μm substrate are used. The plastic material given by Fig. 2(*c*) is used. Since the aspect ratio effect is coupled with the angle effect, 0 deg and 5 deg taper angles are also employed in the following analysis. Equation (15) is used for the stress measurement. As Fig. 9 shows, the aspect ratio generally makes the stress measurement less accurate. The aspect ratio effect is relatively minor for pillars with 0 deg taper angle, and is enlarged for tapered pillars. In fact, the aspect ratio and taper angle have one common effect on stress measurement, namely, the larger they are the less accurate the measured stress.

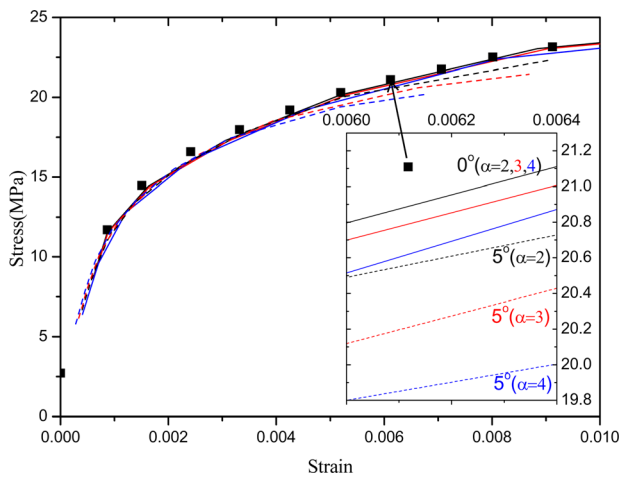

Fig. 9 Aspect ratio effect of stress measurement on plastic pillar using Eq. (15). Black square points are stress-strain input from Fig. 2(*c*).

The reason is related to the radii of the pillars. Both aspect ratio and taper angle contribute to the difference in the pillar top and bottom radii, which causes the inhomogeneous stress state and thus less accurate stress measurement.

5 Concluding Remarks

In this paper, we systematically investigate the stress/strain measurement in the micro-compression test to evaluate the capability of using this test to probe the mechanical properties of both elastic and plastic materials. Regarding the strain measurement, the compliance from the substrate and indenter can be pretty accurately considered by the Sneddon's correction for both elastic and plastic materials. This accuracy does not strongly depend on the shape of the pillar and the size of the substrate. Thus the micro-compression test provides a robust method to measure the strain with quite high accuracy. For the stress measurement, a straight pillar with a 0 deg taper angle is ideal since it can accurately measure the stress. However, for pillars with taper angles, the stress state is not uniform, which is contradictory to the original motivation of using micro-compression test rather than micro-indentation. By defining an empirical means to average out the nonuniform stresses, one can reach pretty accurate stress measurement at certain level of strain.

Overall, the micro-compression test can provide an alternative way to accurately measure strain, and to some extent, stress. Therefore, this test can be used to measure some strain related quantities, such as strain to failure, or the stress-strain relations for plastic materials. Since the pillars with 0 deg taper angles have advantages on both strain and stress measurement, the development of novel fabrication technical to remove the taper angle is desired.

The micro-pillar compression can also be used to probe the size effect. In our experiments that motive this study, we did not observe pronounced size effect. However, some other researchers [11] do observe size effect for the micro-pillars with much smaller size (usually less than 1 μm).

Acknowledgment

The authors are grateful for financial support for this work from the Center for Engineering Materials (CEMAT) at Arizona State University, and the National Science Foundation, Division of Materials Research – Metals Division, DMR-0805144 (Drs. Allan Ardell, Harsh Chopra, and Bruce Macdonald Program Managers). We also appreciate the Fulton High Performance Computing Initiative at Arizona State University for providing computational resources to conduct the simulations.

References

[1] Tabor, D., 2005, *The Hardness of Metals*, Oxford University Press, Oxford, UK.

[2] Uchic, M. D., Dimiduk, D. M., Florando, J. N., and Nix, W. D., 2004, "Sample Dimensions Influence Strength and Crystal Plasticity," Science, **305**(5686), pp. 986–989.

[3] Jiang, L., and Chawla, N., 2010, "Mechanical Properties of Cu6Sn5 Intermetallic by Micropillar Compression Testing," Scripta Mater., **63**(5), pp. 480–483.

[4] Zhang, H., Schuster, B. E., Wei, Q., and Ramesh, K. T., 2006, "The Design of Accurate Micro-Compression Experiments," Scripta Mater., **54**(2), pp. 181–186.

[5] Sneddon, I. N., 1965, "The Relation Between Load and Penetration in the Axisymmetric Boussinesq Problem for a Punch of Arbitrary Profile," Int. J. Eng. Sci., **3**, pp. 47–57.

[6] Frick, C. P., Clark, B. G., Orso, S., Schneider, A. S., and Arzt, E., 2008, "Size Effect on Strength and Strain Hardening of Small-Scale [111] Nickel Compression Pillars," Mat. Sci. Eng. A-Struct., **489**(1–2), pp. 319–329.

[7] Liu, Z. L., Liu, X. M., Zhuang, Z., and You, X. C., 2009, "A Multi-Scale Computational Model of Crystal Plasticity at Submicron-to-Nanometer Scales," Int. J. Plast., **25**(8), pp. 1436–1455.

[8] Akarapu, S., Zbib, H. M., and Bahr, D. F., 2010, "Analysis of Heterogeneous Deformation and Dislocation Dynamics in Single Crystal Micropillars Under Compression," Int. J. Plast., **26**(2), pp. 239–257.

[9] Simmons, G., and Wang, H., 1971, *Single Crystal Elastic Constants and Calculated Aggregate Properties: A Handbook*, MIT Press, Cambridge, MA.

[10] Volkert, C. A., and Lilleodden, E. T., 2006, "Size Effects in the Deformation of Sub-Micron Au Columns," Philos. Mag., **86**(33–35), pp. 5567–5579.

[11] Sun, Q. Y., Guo, Q., Yao, X., Xiao, L., Greer, J. R., and Sun, J., 2011, "Size Effects in Strength and Plasticity of Single-Crystalline Titanium Micropillars With Prismatic Slip Orientation," Scripta Mater., **65**(6), pp. 473–476.